Solving Transient Nonlinear Heat Conduction Problems by Proper Orthogonal Decomposition and the Finite-Element Method

Article *in* Numerical Heat Transfer Fundamentals · August 2005

DOI: 10.1080/10407790590935920

CITATIONS
47

READS
488

3 authors:

Adam Fic
Silesian University of Technology
47 PUBLICATIONS **508** CITATIONS
SEE PROFILE

Ryszard Bialecki
Silesian University of Technology
126 PUBLICATIONS **1,497** CITATIONS
SEE PROFILE

Alain Jacques Kassab
University of Central Florida
239 PUBLICATIONS **2,949** CITATIONS
SEE PROFILE

Numerical Heat Transfer, Part B, 48: 103–124, 2005

ISSN: 1040-7790 print/1521-0626 online
DOI: 10.1080/10407790590935920

Taylor & Francis
Taylor & Francis Group

SOLVING TRANSIENT NONLINEAR HEAT CONDUCTION PROBLEMS BY PROPER ORTHOGONAL DECOMPOSITION AND THE FINITE-ELEMENT METHOD

Adam Fic and Ryszard A. Białecki
Institute of Thermal Technology, Silesian University of Technology, Gliwice, Poland

Alain J. Kassab
Mechanical, Materials and Aerospace Engineering Department, University of Central Florida, Orlando, Florida, USA

A method of reducing the number of degrees of freedom and the overall computing time by combining proper orthogonal decomposition (POD) with the finite-element method (FEM) has been devised. The POD-FEM technique can be applied both to linear and nonlinear problems. At the first stage of the method a standard FEM time-stepping procedure is invoked. The temperature fields obtained for the first few time steps undergo statistical analysis, yielding an optimal set of globally defined trial and weighting functions for the Galerkin solution of the problem at hand. The resulting set of ordinary differential equations (ODEs) is of greatly reduced dimensionality when compared with the original FEM formulation. For linear problems, the set can be solved either analytically, resorting to the modal analysis technique, or by time stepping. In the case of nonlinear problems, only time stepping can be applied. The focus of this article is on the time-stepping approach, in which the generation of the FEM-POD matrices, requiring some additional matrix manipulations, can be embedded in the assembly of standard FEM matrices. The gain in execution times comes from the significantly shorter time of solution of the set of algebraic equations at each time step. Numerical results are presented for both linear and nonlinear problems. In the case of linear problems, the derived time-stepping technique is compared with the standard FEM and the modal analysis. For nonlinear problems the proposed POD-FEM approach is compared with the standard FEM. Good accuracy of the POD-FEM solver has been observed. Controlling the error introduced by the reduction of the degrees of freedom in POD is also discussed.

Received 3 December 2004; accepted 30 December 2004.

This work was supported by the National Committee for Fundamental Research, Poland, under grant 135/E-367/SPB/5.PR UE/DZ 348.

A preliminary version of the article was presented at CHT-04: An ICHMT International Symposium on Advances in Computational Heat Transfer, April 2004, G. de Vahl Davis and E. Leonardi (eds.), CD-ROM Proceedings, ISBN 1-5670-174-2, Begell House, New York, 2004.

Address correspondence to Adam Fic, Institute of Thermal Technology, Silesian University of Technology, Konarskiego 22, 44-100 Gliwice, Poland. E-mail: fic@itc.polsl.pl

NOMENCLATURE

$\mathbf{C}$	covariance matrix of snapshots	$\hat{\mathbf{T}}$	column vector of unknowns after POD transformation
$\mathbf{F}$	load (right-hand-side) vector	$\mathbf{U}$	matrix of snapshots
$\mathbf{I}$	unit square matrix	$\mathbf{v}$	eigenvector
K	number of reduced DOFs in POD	$\mathbf{V}$	matrix collecting eigenvectors (modal matrix)
$\mathbf{K}$	conductance (stiffness) matrix	$\hat{\mathbf{w}}$	column vector of global weighting functions
L	number of snapshots	λ	eigenvalue
$\mathbf{M}$	capacitance (mass) matrix	$\mathbf{\Phi}$	POD basis matrix
N	number of nodes	$\hat{\mathbf{\Phi}}$	truncated POD basis matrix
$\mathbf{N}$	column vector of shape functions		
$\hat{\mathbf{N}}$	column vector of global trial functions		

1. INTRODUCTION

The accuracy of numerical simulation depends strongly on the density of the mesh used when discretizing the boundary-value problem at hand. Fine grids produce trustworthy solutions, but the price is an increased number of degrees of freedom (DOFs), leading to long computing times and high storage requirements. In many problems, specifically when real-time solutions are required, the need to accelerate the calculations is vital. There has been constant progress in the acceleration of solution procedures. The repertoire of means used to reach this goal is broad: parallelization, multigrid iterative solvers, domain decomposition, to name only a few.

This article deals with another possibility for reducing the overall computing time by reducing the number of DOFs of the original discretized problem. The rationale for this approach is as follows. Consider a spatial field (temperature) that depends on one parameter (time). It is obvious that the temperature fields corresponding to a sequence of time instants are mutually correlated. The information concerning the interrelation of the fields can be extracted using statistical methods. This knowledge can then be used to reduce the number of degrees of freedom necessary to describe the spatial distribution of temperature.

Statistics offer an efficient technique for detecting the correlations present in large data sets. The technique is known as proper orthogonal decomposition (POD) and goes under several other names as well. Basic features of the method are discussed in the next section. It is enough to mention here that POD can be seen as a technique for approximating a set of vectors using a rotated orthogonal coordinate frame. The angles of rotation are selected in such a way that the projections of the vectors on subsequent coordinate axes decay in the most rapid way. Thus, only the few first projections are needed to approximate all vectors constituting the set. The directions of the rotated coordinates axes are termed the POD basis.

If the original set of the vectors comes from a solution of a boundary-value problem, another interpretation of POD is possible. In this case the POD basis is a discrete approximation of the set of eigenfunctions of the boundary-value problem at hand. As eigenfunctions constitute the best possible basis of approximation, only the first few terms are needed to achieve good accuracy of representation of the field under consideration.

The idea of using POD in the context of time-dependent numerical solution (primarily the finite-element method, FEM) is not new. It has been exploited in the literature in structural dynamics [1] and in aeroelastic [2] and fluid dynamics [3]. Standard time-stepping procedure has been used in all these articles.

The present article is an extension of our previous work [4, 5] in which the POD FEM combination has been used for solving transient linear heat conduction problems using modal analysis. The procedure proved to be very effective. For example, when solving a 3-D unsteady linear heat conduction problem in a radiator (51,897 nodes) with constant boundary conditions, the number of DOFs was reduced to 20, and the maximal error was less than 0.8%. The overall computing time was 10 times shorter than when using the standard FEM.

The focus in the present paper is on solving *nonlinear transient heat conduction problems*. The nonlinearity excludes the application of modal analysis. Thus, the resulting set of ODEs has to be solved using time stepping. Although any discretization method can be applied to generate the ODEs (finite differences, finite volumes, finite elements, boundary elements, or meshless techniques), the analysis in this article is FEM-oriented.

The execution-time economy in the POD-FEM comes in this case from the significant drop in the computational time of the equation solver coming from the reduction of DOFs. On the other hand, the time of POD-FEM matrix assembly is greater than for its standard counterpart. As a result, overall saving in execution time can be expected only for very large problems. This article proposes a technique for accelerating the POD-FEM assembly process designed for the case when the entire stiffness matrix needs to be recomputed at every time step. Using this approach, the gains by using the POD-FEM can be seen even for small problems. The crucial point of the procedure is the evaluation of the POD set. The next section is devoted to this problem.

2. FUNDAMENTALS OF PROPER ORTHOGONAL DECOMPOSITION

POD is a technique for extracting information from empirical data. Using statistical methods, the correlations among a sequence of data sets are detected. The POD basis is optimal in the sense that the first terms contain more *energy* than the same number of terms of any other basis. Thus, POD has been used to obtain models which capture the overall behavior of a physical system using a reduced number of degrees of freedom.

Determination of the optimal basis requires some additional computational effort. However, as will be shown, the cost of these calculations is low. This article describes a variant of the POD known as the snapshot method, which was developed by Sirovich [6]. An alternative approach is to use the singular value decomposition technique to construct the POD basis. Reference [7] shows the equivalence of three different POD variants: principal component analysis, Karhunen-Loeve decomposition, and singular value decomposition. The technique is also known under several other names, such as Hotteling transformation, quasiharmonic modes, empirical orthogonal functions, etc. The nonuniform terminology comes from the fact that POD has been reinvented several times and used in surprisingly many fields of science and technology.

The literature on the subject is vast, and this article makes no attempt to give a complete review of the relevant references. The method was developed about 100 years ago [8]. Since then, it has been used as a tool for processing statistical data [9–11], pattern recognition, e.g., characterization of human faces [12], and control theory [13]. Another important area of application of POD technique is in turbulence, where this method has been used to detect large-scale organized spatial motions [14]. In acoustical and random signal decomposition, POD has been applied to extract information about the modes and energy of the signals under consideration [15]. This feature is very useful in applications that involve compression and storage of stochastic signals [16]. The analysis of the activity of the visual cortex in a turtle brain [17] is an example of application of POD in bioengineering. POD has also been successfully applied to inverse problems [18] exhibiting strong regularization properties.

The fundamental notion of POD is the *snapshot*, being a collection of N sampled values of the field under consideration. The snapshot is stored in a vector (column matrix) $\mathbf{U}^i$, $i = 1, 2, \ldots, L$. A collection of all snapshots is a rectangular $N \times L$ matrix $\mathbf{U}$. The snapshots are generated by changing the values of some parameter(s) on which the field depends. In the transient problems discussed in this article, the natural choice of such a parameter is the time variable.

The snapshots may be obtained either from a mathematical model of the phenomenon or from experiments. The aim of POD is to construct a set of vectors (basis) $\mathbf{\Phi}^j$ resembling the original matrix $\mathbf{U}$. The basis is stored in another rectangular matrix $\mathbf{\Phi}$ of the same dimensionality as $\mathbf{U}$. The sought-for basis is orthogonal, i.e.,

$$\mathbf{\Phi}^T\mathbf{\Phi} = \mathbf{I}(L) \tag{1}$$

where the superscript T denotes the transpose and $\mathbf{I}(L)$ is the unit matrix of dimension L. The basis matrix also fulfills the adjoint orthogonality condition

$$\mathbf{\Phi}\mathbf{\Phi}^T = \mathbf{I}(N) \tag{2}$$

From basic linear algebra it follows immediately that the snapshots can be expressed in the basis as

$$\mathbf{U} = \mathbf{\Phi}\mathbf{a} \tag{3}$$

where $\mathbf{a}$ is a square matrix of coefficients of the expansion, whose entries can be calculated by taking advantage of the orthogonality condition (1) as

$$\mathbf{a} = \mathbf{\Phi}^T\mathbf{U} \tag{4}$$

The snapshot matrix can be approximated using a truncated basis matrix $\hat{\mathbf{\Phi}}(K)$ of $K < L$ columns,

$$\mathbf{U} \approx \hat{\mathbf{\Phi}}(K)\hat{\mathbf{a}} \tag{5}$$

where $\hat{\mathbf{a}}$ is the truncated coefficients matrix.

While the truncated basis matrix still satisfies the orthogonality condition,

$$\hat{\mathbf{\Phi}}^T(K)\hat{\mathbf{\Phi}}(K) = \mathbf{I}(K) \tag{6}$$

it does not fulfill the adjoint orthogonality,

$$\hat{\mathbf{\Phi}}(K)\hat{\mathbf{\Phi}}^T(K) \neq \mathbf{I}(N) \tag{7}$$

Taking advantage of the orthogonality of the truncated POD basis (6), the truncated matrix of coefficients can be evaluated from the relationship

$$\hat{\mathbf{a}} = \hat{\mathbf{\Phi}}^T\mathbf{U} \tag{8}$$

There is an infinite number of orthogonal bases and the task is to select one exhibiting optimal approximation property. Let ε be the error of the approximation defined as

$$\varepsilon = \left\|\mathbf{U} - \hat{\mathbf{\Phi}}(K)\hat{\mathbf{a}}\right\| = \left\|\mathbf{U} - \hat{\mathbf{\Phi}}(K)\hat{\mathbf{\Phi}}^T(K)\mathbf{U}\right\| \tag{9}$$

The goal is to find a truncated, orthonormal basis that for a prescribed error level ε has a minimum number of columns K. This condition is supplemented by an additional requirement, that the basis is expressed as a linear combination of snapshots, i.e.,

$$\hat{\mathbf{\Phi}}(K) = \mathbf{U}\hat{\mathbf{V}} \tag{10}$$

where $\hat{\mathbf{V}}$ is a rectangular matrix comprised of L rows by K columns. By introducing the latter condition, finding the optimal basis $\hat{\mathbf{\Phi}}$ has been recast into the problem of evaluating a much smaller matrix $\hat{\mathbf{V}}$.

It can be shown [8] that the constraint optimum problem posed by (9) and (10) is equivalent to the following eigenvalue problem:

$$\mathbf{C}\mathbf{v} = \lambda\mathbf{v} \tag{11}$$

where

$$\mathbf{C} = \mathbf{U}^T\mathbf{U} \tag{12}$$

is the covariance matrix, and the following solutions, i.e., eigenvectors $\mathbf{v}_i$, are associated with eigenvalues λ_i ($i = 1, 2, \ldots, L$) of the problem (11). The eigenvectors are by definition orthogonal and can be scaled to satisfy a condition

$$\mathbf{v}_i\mathbf{v}_j = \frac{\delta_{ij}}{\lambda_i} \tag{13}$$

where Kronecker symbol $\delta_{ij} = 1$ if $i = j$ and $\delta_{ij} = 0$ if $i \neq j$.

As matrix $\mathbf{C}$ is positive definite and symmetric, the eigenvalues are positive and real. It is convenient to calculate them in decreasing order. The truncated modal

matrix $\hat{\mathbf{V}}$ is now defined as a collection of the first K eigenvectors stored as columns of the matrix.

Calculation of the full spectrum of the covariance matrix $\mathbf{C}$ may lead to long computing times. Some economy can be achieved by limiting the number of evaluated eigenvalues and eigenvectors. In the present work this has been accomplished using an ISML routine, DEVFSF [19], in which only the largest eigenvalues (belonging to a predefined interval) are evaluated.

From the orthogonality condition (13), it follows immediately that the truncated modal matrix is indeed orthogonal:

$$\hat{\mathbf{V}}^T\hat{\mathbf{V}} = \mathbf{\Lambda}^{-1}(K) \tag{14}$$

where $\mathbf{\Lambda}^{-1}(K)$ is a diagonal matrix whose entries are defined as $\{\mathbf{\Lambda}^{-1}\}_{ii} = 1/\lambda_i$. The truncated modal matrix satisfies the condition

$$\hat{\mathbf{V}}^T\mathbf{C}\hat{\mathbf{V}} = \mathbf{I}(K) \tag{15}$$

A consequence of the latter property is the orthogonality of the truncated basis,

$$\hat{\mathbf{\Phi}}^T\hat{\mathbf{\Phi}} = \left(\mathbf{U}\hat{\mathbf{V}}\right)^T\left(\mathbf{U}\hat{\mathbf{V}}\right) = \hat{\mathbf{V}}^T\mathbf{C}\hat{\mathbf{V}} = \mathbf{I}(K) \tag{16}$$

POD can be interpreted as a decomposition of the field into a set of approximating functions (eigenfunctions). Thus the technique is sometimes referred to as the *empirical eigenfunctions* method. In view of this, Eqs. (3) and (5) are discrete analogs of Fourier expansion of the field into uncorrelated modes.

If velocity is the field under consideration, it can be shown [20] that the kinetic energy corresponding to a given mode (eigenvector) is equal to the associated eigenvalue. In this case, the error introduced by working with the truncated basis has a simple physical interpretation. The total energy of the field is equal to the sum of eigenvalues in the complete POD basis. The energy associated with the first K POD eigenmodes is equal to the sum of the first K eigenvalues. The ratio of these two sums of eigenvalues defines the fraction β of energy included in the truncated basis.

Reference [1] gives an alternative interpretation of POD for structural problems. Here the POD modes are interpreted in terms of polar moments of inertia. For other fields the physical interpretation of POD is not that obvious, but in any case the eigenvalues of the covariance matrix are the measure of importance of a given POD mode.

As the snapshots are generated by sampling some physical fields, they are mutually interrelated. Rapid decay of subsequent eigenvalues indicates a strong correlation of the snapshots giving rise to the reduction of the necessary DOFs to describe the behavior of the field. In typical applications, only the few first eigenvalues are significant. The modes whose energy is at the level of computer accuracy can be neglected without loss of accuracy.

3. COMBINED POD-FEM NUMERICAL TECHNIQUE

3.1. Time-Stepping Approach

A transient nonlinear heat conduction problem is considered. The standard FEM procedure leads to a set of N ODEs of the form

$$\mathbf{M}(\mathbf{T})\dot{\mathbf{T}} + \mathbf{K}(\mathbf{T})\mathbf{T} = \mathbf{F}(\mathbf{T}) \tag{17}$$

where $\mathbf{T}$ is the vector of unknown nodal temperatures, $\dot{\mathbf{T}}$ denotes the vector of their temporal derivatives, $\mathbf{M}$ stands for the capacitance (mass) matrix, $\mathbf{K}$ denotes the conductance (stiffness) matrix, and $\mathbf{F}$ is the right-hand-side (load) vector.

The entries of the stiffness and mass matrices are evaluated by integration over the volume of the computational domain. Influence of the boundary conditions is accounted for by performing integration over the boundary, which is much cheaper than volume integration. Therefore, for nonlinear cases, the worst possible scenario is when material properties are solution-dependent. In such a case, the entries of stiffness, mass matrices, and elements of the load vector are solution-dependent. As opposed to the linear case, the matrices cannot be reused at the next time step and should be recomputed at every time step.

The procedure starts with a solution of the problem by the standard FEM. The set of equations (17) is solved using an (implicit or explicit) time-stepping procedure. The process is terminated after executing the first L time steps. Subsequent vectors $\mathbf{U}^i = \mathbf{T}^i$ ($i = 1, 2, \ldots, L$) of all resulting nodal temperatures (snapshots) collected in columns of matrix $\mathbf{U}$ are used to calculate the symmetric and positive-definite covariance matrix $\mathbf{C}$ [Eq. (12)], whose subsequent eigenvectors are used to determine the truncated POD basis $\hat{\mathbf{\Phi}}$ of N rows and K columns, as described in the previous section.

Because of the strong snapshots correlation, the decay of the eigenvalues of the covariance matrix is rapid. As a result, only the first few K modes are needed to define the truncated POD basis $\hat{\mathbf{\Phi}}$. Once the basis is known, the temperature field can be approximated with acceptable accuracy by

$$\mathbf{T} = \hat{\mathbf{\Phi}}\hat{\mathbf{T}} \tag{18}$$

The column vector $\hat{\mathbf{T}}$ is here a collection of new unknowns. The dimensionality of this vector is reduced to K elements, which is significantly less than the number of nodes N.

The Galerkin method can be employed now to formulate the system of equations in terms of the set of new unknowns collected in vector $\hat{\mathbf{T}}$. The trial and weighting functions are then defined as a linear combination of shape functions. Thus, the global trial functions collected in vector $\hat{\mathbf{N}}(\mathbf{x})$ of dimension K are determined as

$$\hat{\mathbf{N}}^T(\mathbf{x}) = \mathbf{N}^T(\mathbf{x})\hat{\mathbf{\Phi}} \tag{19}$$

where $\mathbf{x}$ stands for the coordinate vector and $\mathbf{N}(\mathbf{x})$ is the N-dimensional column vector of standard shape functions. The column vector of the weighting functions $\hat{\mathbf{w}}(\mathbf{x})$ is defined as follows:

$$\hat{\mathbf{w}}(\mathbf{x}) = \hat{\mathbf{\Phi}}^T\mathbf{N}(\mathbf{x}) \tag{20}$$

The approach is equivalent to transformation of the system (17) by its left-sided multiplication by $\hat{\mathbf{\Phi}}^T$ and substitution of (18), which results in

$$\hat{\mathbf{M}}\dot{\hat{\mathbf{T}}} + \hat{\mathbf{K}}\hat{\mathbf{T}} = \hat{\mathbf{F}} \tag{21}$$

where

$$\hat{\mathbf{M}} = \hat{\mathbf{\Phi}}^T \mathbf{M} \hat{\mathbf{\Phi}} \tag{22}$$

$$\hat{\mathbf{K}} = \hat{\mathbf{\Phi}}^T \mathbf{K} \hat{\mathbf{\Phi}} \tag{23}$$

$$\hat{\mathbf{F}} = \hat{\mathbf{\Phi}}^T \mathbf{F} \tag{24}$$

$\hat{\mathbf{M}}$ and $\hat{\mathbf{K}}$ are now symmetric, fully populated $K \times K$ matrices. System (21) is solved using an implicit time-stepping procedure, which leads to the $K \times K$ system of algebraic equations of form:

$$\mathbf{A}\hat{\mathbf{T}} = \mathbf{B} \tag{25}$$

Inverse transformation is defined by Eq. (18).

As mentioned previously, the aim of using the POD technique combined with the FEM is reduction of the number of DOFs, but the primary goal is to reduce the computing time. The cost of FEM solution consists, roughly speaking, of two components: matrix generation and solution of equations. As the dimensions of the POD-FEM matrices $\hat{\mathbf{K}}$ and $\hat{\mathbf{M}}$ are much lower than their standard FEM counterparts, the time required to solve the equation set (25) is much less than for the original FEM system. On the other hand, matrix generation in POD-FEM is considerably more expensive than in the case of the standard FEM. The reason for this is clear. As can be seen from Eqs. (22) and (23), generation of POD-FEM matrices requires two additional matrix multiplications. Evaluation of the POD-FEM matrices at every time step directly from Eqs. (22) and (23) would lead to prohibitively long computing times. Thus, the approach used in the study was to separate the solution-dependent part of the element matrix from the geometry-dependent one. The procedure for assembling the final POD-FEM stiffness matrix consists of the following steps:

At the first step, the FEM element matrices $\mathbf{K}_{1e}$ are determined. These are the standard FEM element matrices evaluated taking the conductivity value equal to 1.

For every FEM element matrix, the POD-FEM element matrix $\hat{\mathbf{K}}_{1e}$ is calculated and stored. This was done making use of the equation

$$\hat{\mathbf{K}}_{1e} = \hat{\mathbf{\Phi}}_e^T \mathbf{K}_{1e} \hat{\mathbf{\Phi}}_e \tag{26}$$

where matrices $\hat{\mathbf{\Phi}}_e$ collect only the appropriate rows of matrix $\hat{\mathbf{\Phi}}$ referred to the following nodes of element e. Thus, advantage has been taken of the sparsity of the element stiffness matrix $\mathbf{K}_{1e}$.

In the following time steps, the global POD-FEM matrix $\hat{\mathbf{K}}$ is assembled as

$$\hat{\mathbf{K}} = \sum_{e=1}^{NE} k_e \hat{\mathbf{K}}_{1e} \tag{27}$$

where NE stands for the total number of volumetric elements and k_e is the average conductivity for element e. It should be stressed that only these values of the conductivity undergo changes in subsequent time steps.

Strictly speaking, the heat conductivity should be sampled at each Gaussian node, but averaging of the material property introduces insignificant error while greatly speeding up the calculations. Therefore, material property averaging is popular among programmers. To provide a fair comparison of the FEM and POD-FEM, material property averaging has also been used in all reference FEM solutions reported in the results section.

The volumetric contributions to both the mass matrix and load vector can be evaluated using an analogous procedure. Comparison of the execution times for POD-FEM and the standard FEM is shown in the next section. It should be stressed that material properties averaging has been applied in both cases.

3.2. Modal Approach for Linear Problems

For linear problems, an alternative POD-FEM technique can be applied for solving transient heat conduction problems. This approach is applicable for both constant and time-dependent loads [4, 5]. The first step is the generation of ODEs (17) using the classical FEM approach. An outline of the method is described below. It is assumed that the lumped formulation of capacitance matrix is used.

For linear problems, the set of equations of form (17) can be solved using the concept of modal decomposition analysis [21]. This method is an analytical solution of the set of equations (17) with respect to time. The crucial stage of this approach is the determination of the eigenvalues and eigenvectors of the transformed stiffness matrix in the case of the problem considered. It is therefore convenient to have this matrix symmetric, as then the eigenvalues are real. To preserve the symmetry of the transformed stiffness matrix, system (17) should be transformed defining a new variable $\mathbf{T}^*$:

$$\mathbf{T} = \mathbf{M}^{-1/2}\,\mathbf{T}^* \tag{28}$$

where $\mathbf{M}^{-1/2}$ is an $N \times N$ diagonal matrix determined as $\left\{\mathbf{M}^{-1/2}\right\}_{ii} = 1/\sqrt{m_{ii}}$, with m_{ii} denoting the ith diagonal term of the diagonal capacitance matrix $\mathbf{M}$.

Substitution of (28) into (17) and multiplying the result by $\mathbf{M}^{-1/2}$ yields a set of N ODEs of form

$$\dot{\mathbf{T}}^* + \mathbf{K}^*\,\mathbf{T}^* = \mathbf{F}^* \tag{29}$$

where $\mathbf{K}^* = \mathbf{M}^{-1/2}\,\mathbf{K}\mathbf{M}^{-1/2}$ is a symmetric sparse matrix, and $\mathbf{F}^* = \mathbf{M}^{-1/2}\,\mathbf{F}$. The POD technique comes to play at the next step. Transformation

$$\mathbf{T}^* = \hat{\mathbf{\Phi}}\hat{\mathbf{T}} \tag{30}$$

similar to (18), leads to the system of form (21), with slightly redefined matrices: $\hat{\mathbf{M}} = \mathbf{I}(K)$, $\hat{\mathbf{K}} = \hat{\mathbf{\Phi}}^{\mathbf{T}}\,\mathbf{K}^*\,\hat{\mathbf{\Phi}}$, and $\hat{\mathbf{F}} = \hat{\mathbf{\Phi}}^{\mathbf{T}}\,\mathbf{F}^*$. Matrix $\hat{\mathbf{K}}$ is a fully populated $K \times K$ symmetric matrix, and the number K of new unknowns collected in vector $\hat{\mathbf{T}}$ is significantly smaller than the original number of nodes N. Thus, the solution of the resulting ODEs can be accomplished by modal decomposition with significant gain in computing times [4, 5]. Inverse transformation is more complex than in the case of the time-stepping approach. However, the transformation matrix linking the modal solution and the original temperature field $\mathbf{T}$ needs to be determined only once [5].

It should be pointed out that the snapshots in the case of the modal approach of POD-FEM considered are not just the nodal temperatures. The covariance matrix is generated using the vectors of nodal temperatures scaled by the mass matrix entries, i.e., $\mathbf{U}^i = \mathbf{T}^{*i}$ ($i = 1, 2, \ldots, L$).

3.3. Errors Introduced by POD Truncation

The quantity of direct interest is the error in temperature introduced by the POD approximation. To investigate how the error develops with time, two relative error definitions at a given time instant t are introduced: the average error $\delta_m(t)$ and the local error $\delta_T(t)$. These errors are expressed in terms of three quantities: the absolute error δT_i of the temperature at node i, the excess ΔT_i of temperature over the initial condition at a given node, and, the mean excess of temperature $\Delta T_m = \sum_{i=1}^{N} \Delta T_i / N$. The average global error is defined as

$$\delta_m(t) = \frac{\sum_{i=1}^{N} \delta T_i}{N \Delta T_m} \tag{31}$$

while the measure of the local one is

$$\delta_T(t) = \max_i \left(\frac{\delta T_i}{\Delta T_i} \right) \tag{32}$$

The standard FEM solution has been treated as a reference solution to which the POD-FEM results are benchmarked in every case reported in the example section.

4. NUMERICAL EXAMPLES

A 2-D gas-cooled turbine blade was considered. The geometry and the imposed boundary conditions are shown in Figure 1. The initial condition was a constant temperature $T_0 = 300\,\mathrm{K}$. The temperatures of both the coolant and the working fluid changed in time. The initial coolant temperature was equal to the initial temperature

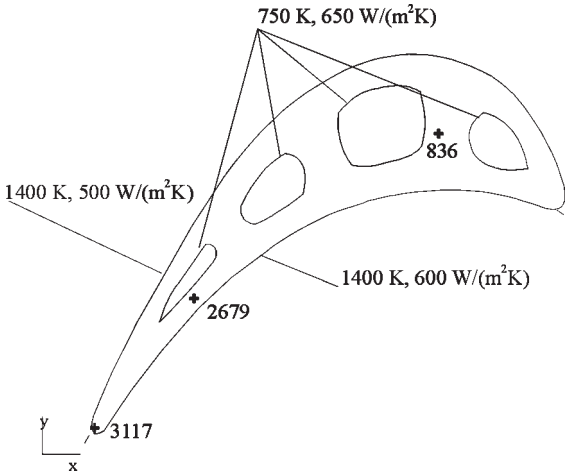

Figure 1. Geometry of the blade, boundary conditions, and location of selected nodes.

of the blade, i.e., 300 K. Then, the temperature of coolant changed linearly in time, reaching 750 K after 150 s. After this time, the coolant temperature remained constant. The temperature of the working fluid changed exponentially as $T_f = 300 + 1{,}100\ [1 - \exp(-t/80)]$, where t denotes time in seconds.

The problem has been solved using an in-house FEM package based on FEAP [21] equipped with a time-stepping POD-FEM option and in-house code based on the described modal POD-FEM technique. The numerical mesh consisted of 4-node isoparametric elements.

4.1. LINEAR PROBLEM: EXAMPLE 1

Comparison of the results obtained by the time-stepping and modal approaches of the POD-FEM is the purpose of investigations presented in this subsection. The values of the material properties used in the example were: heat conductivity $k = 22\,\mathrm{W/m\,K}$, specific heat capacity of a unit volume $c_p = 3.67\,\mathrm{MJ/m^3K}$. The numerical mesh consisted of 3,151 nodes.

After generating 200 snapshots using a time step of 0.1 s and central differences, the POD basis has been generated. The fraction β of neglected energy was of the order of 5E-12. The full set has been limited to 16 degrees of freedom (recall that the original set contained 3,151 unknowns) using the modal version of POD-FEM, and to 11 DOFs for the time-stepping approach. The eigenvalues of the covariance matrix decreased very rapidly in both versions, suggesting strong interrelation of the snapshots (cf. Figure 2). However, in the modal POD-FEM, the interrelation is slightly worse. This can be explained by the fact that for the modal analysis the snapshots are defined as scaled temperatures $\mathbf{T}^*$ [Eq. (22)], i.e., quantities with no physical meaning. The snapshots used in the time-stepping POD-FEM approach are defined as vectors of nodal temperature, and as such have direct physical meaning.

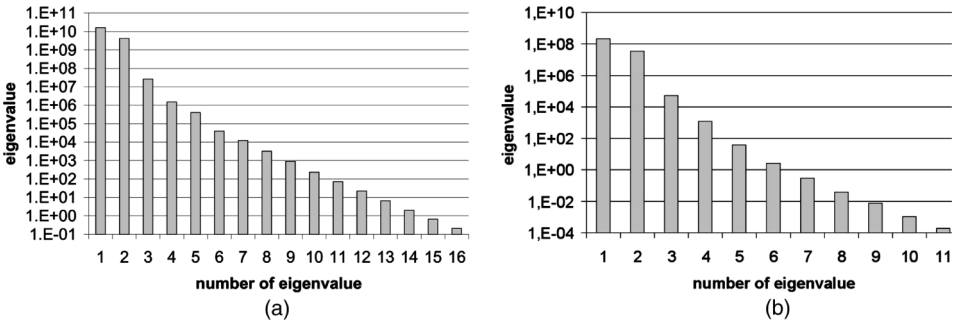

Figure 2. Distribution of eigenvalues of the covariance matrix for the linear problem: (*a*) modal approach; (*b*) time-stepping approach.

The changes of temperature at three characteristic nodes marked in Figure 1 obtained using the time-stepping POD-FEM, as well as changes of fluid temperatures, are shown in Figure 3. The accuracy of the modal solution at node

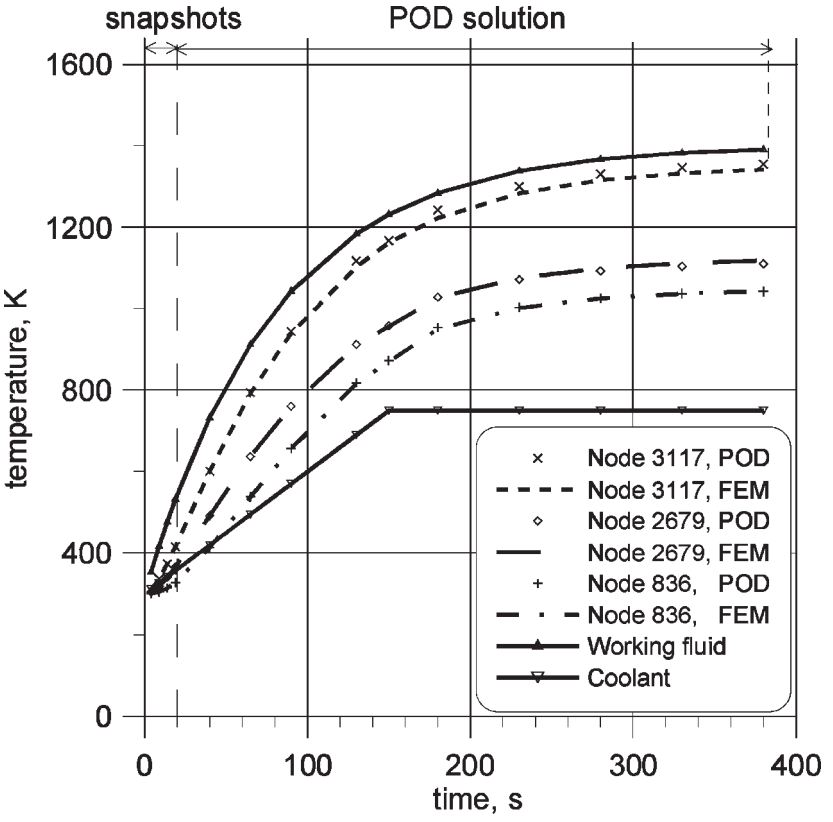

Figure 3. Fluid temperatures and resulting temperatures at selected nodes for linear problem using time-stepping POD-FEM.

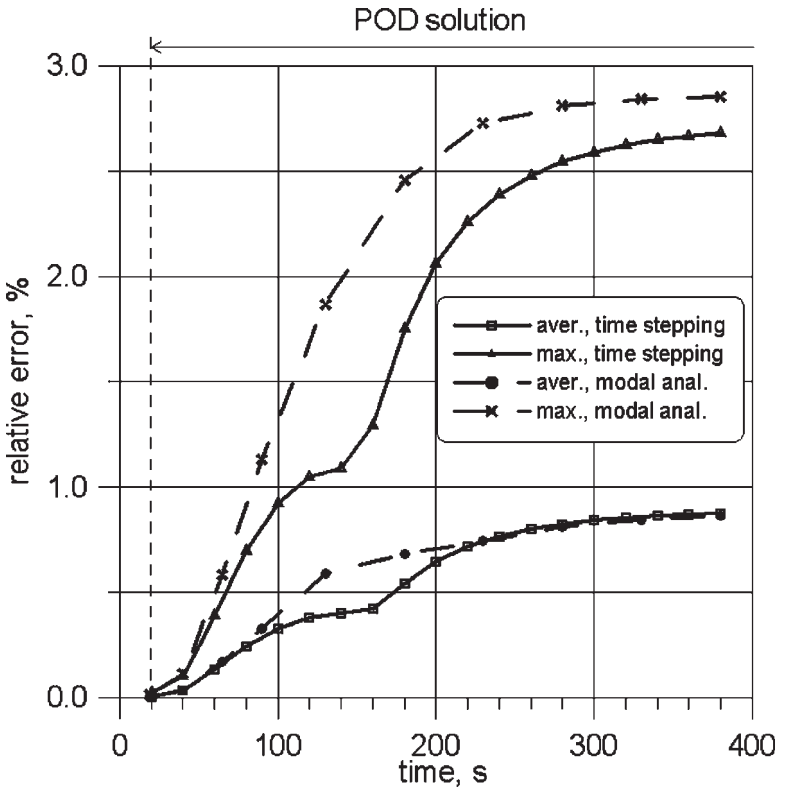

Figure 4. Comparison of errors for the linear problem solved by modal and time-stepping POD-FEM.

3,117 was the worst among all nodal points. These nodal temperatures are compared with the standard FEM results. The temporal variation of errors of the temperature for the time-stepping and modal POD-FEM is presented in Figure 4.

It should be noticed that the maximal error does not exceed 3%, and the average error 0.8%. The time-stepping POD-FEM yields results comparable with the modal POD-FEM, and maximal error is even smaller in this case. The errors reach their maximum in an asymptotic way, not exceeding it. The time interval used to generate the snapshots was of the order of 20 s, while the POD solution has been generated for times one order of magnitude larger.

4.2. Nonlinear Problem: Example 2

In the second example the source of the nonlinearity was the temperature-dependent heat conductivity. The value of conductivity was $k = 40\,\mathrm{W/m\,K}$ at 300 K, $k = 20\,\mathrm{W/m\,K}$ at 1,500 K, with linear dependence of the conductivity on temperature between these two temperatures. Remaining assumptions were the same as in Example 1. The problem was solved using the time-stepping POD-FEM. The numerical mesh consisted of 3,151 nodes.

Two hundred snapshots were also generated using a time step of 0.1 s. Although the fraction β of neglected "energy" was slightly higher than previously and equal to 1E-11, the resulting dimensionality of the POD basis was larger (31) than in the linear case (16). This suggests that the interrelation of snapshots is worse than in the linear case. The eigenvalues of the covariance matrix are shown in Figure 5. Rapid decay of their values proves a strong correlation between the snapshots. Figure 6 shows the comparison of the *exact* FEM solution with the time-stepping POD-FEM results. As the eigenvalues (Figure 5) from about the 11th are almost constant and very small, the problem was recalculated using lower values of DOFs (number of modes K of the truncated POD basis $\hat{\mathbf{\Phi}}$). The errors, defined by Eqs. (31) and (32), are, for the case under consideration, depicted in Figure 7. Results obtained using 31 and 11 DOFs ($\beta = 1.5\text{E-}11$) were practically the same. Further reduction of DOFs up to 7 ($\beta = 1\text{E-}09$) did not incur significant loss of accuracy. If 6 DOFs ($\beta = 0.9\text{E-}09$) were used, the errors magnified notably and, referred to the time instant 380 s, the maximum relative error achieved 6.97%, while the average was 1.98%.

It can be seen that the material nonlinearity considered does not introduce additional error when compared to the linear case.

It is worth noting that the POD-FEM technique does not work correctly when degenerated triangle elements (quadrangles with double nodes) are used.

4.3. Nonlinear Problem: Example 3

The third problem considered was similar to Example 2, but the numerical mesh consisted of 37,732 nodes. Moreover, the heat capacity per unit volume was assumed to be temperature-dependent. Its value was $c_p = 3.5\,\mathrm{MJ/m^3\,K}$ at 300 K, and $c_p = 5.0\,\mathrm{MJ/m^3\,K}$ at 1,500 K, with linear dependence on temperature between these two temperatures. As a result, the capacitance matrix had to be recalculated in each time step. The remaining assumptions were the same as in Example 2.

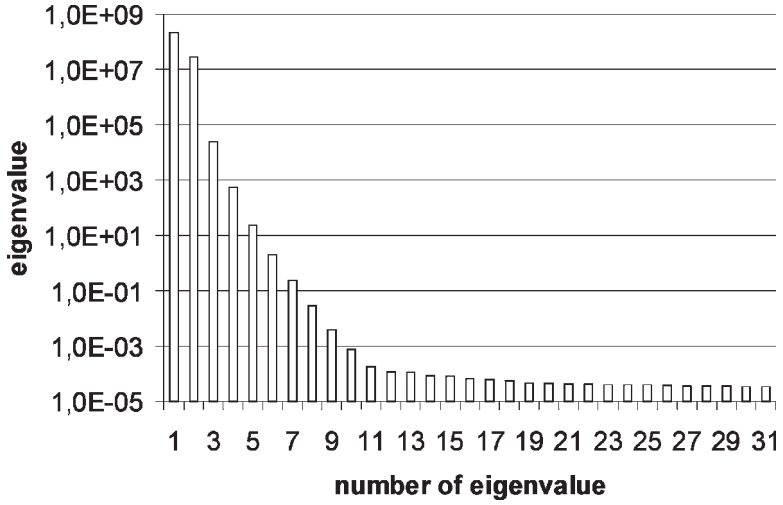

Figure 5. Distribution of eigenvalues of the covariance matrix for Example 2.

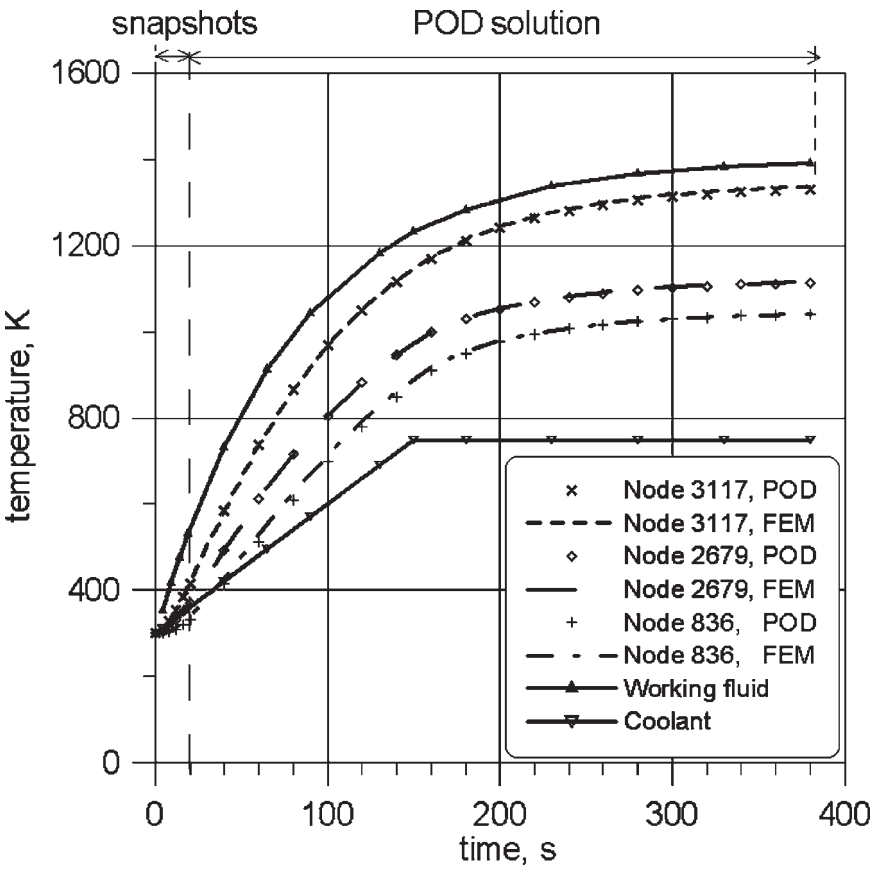

Figure 6. Fluid temperatures and results at selected nodes for Example 2.

Two hundred snapshots were also generated in this example using a time step of 0.1 s. The eigenvalues of the covariance matrix are shown in Figure 8. The neglected "energy" fraction β was higher than the previously assumed value and equal to 8E-11. The resulting dimensionality of the POD basis was 21. Comparative calculations using the standard FEM and the time-stepping POD-FEM was carried out employing a POD basis consisting of 6 through 21 modes. It can be seen that the eigenvalues starting from the 10th were 10 orders of magnitude higher than the first one. The errors of the POD-FEM results in the cases considered are shown in Figure 9. Accuracy of results obtained using 21 and 8 DOFs ($\beta = 2E\text{-}10$) was practically the same. Further reduction of DOFs reduced the accuracy. For 6 DOFs ($\beta = 1E\text{-}08$) the maximum relative error assumed the value of 3.09%, while the average was 0.93% for the time instant 380 s.

It should be pointed out that although the number of nodes used in this example was more than 10 times higher than in Example 2, the number of POD modes required to keep the error at an acceptable level was practically the same.

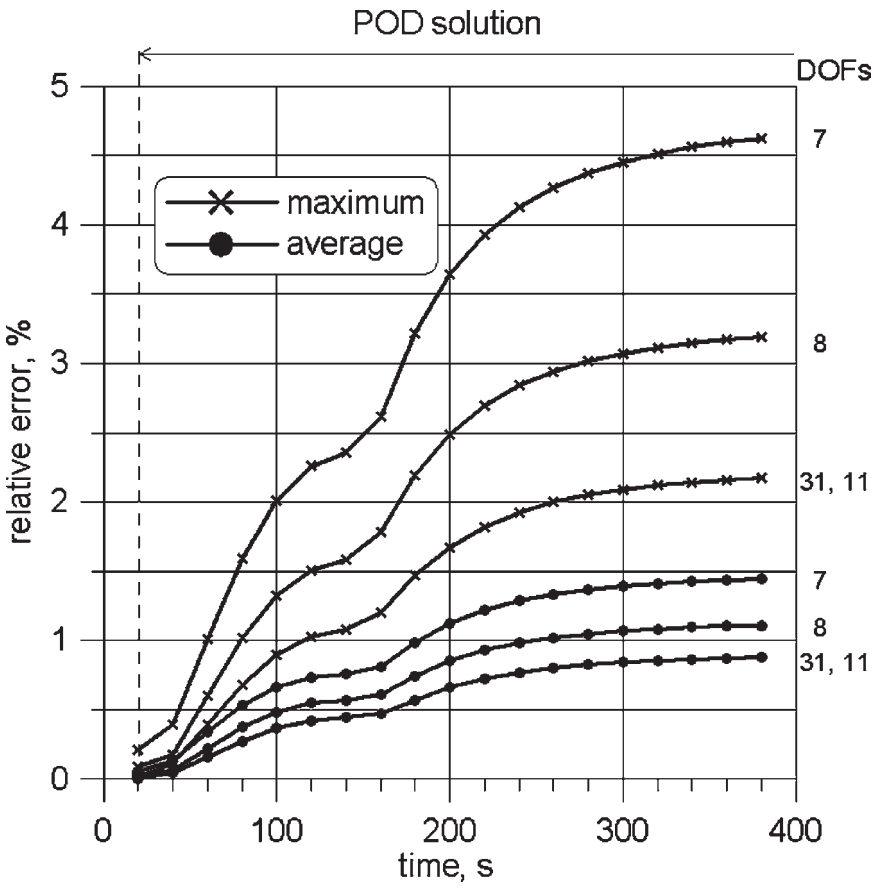

Figure 7. Errors of results obtained for Example 2 when POD basis with different values of DOFs was used. Numbers on the right margin indicate the numbers of DOFs.

4.4. Computing Times

Simplified operation count shows that the execution time of the equation solver depends on the square of the number of DOFs $O(N^2)$ [1] for the FEM matrix (in-core skyline solver) and the cube of the number of POD modes $O(K^3)$ in the POD-FEM case (standard symmetric Gauss solver). The assembly time is proportional to the number of DOFs in standard FEM $O(N)$, while the assembly of the POD-FEM system is of order $O(NK^2)$ and as such is of order of $O(K^2)$ more expensive. The latter tendency has been checked empirically. Figure 10 shows the dependence of the assembly time for the exact (left) and simplified version of entries evaluation of the POD-FEM matrix arising in Example 2. It can be seen that the assembly time is in both cases proportional to the squared number of POD modes K.

The POD-FEM reduces total execution times only in the case of large problems, where the solution time dominates. For the code used in our examples, the limit was about 3,000–4,000 DOFs. When compared to the stiffness matrix assembly

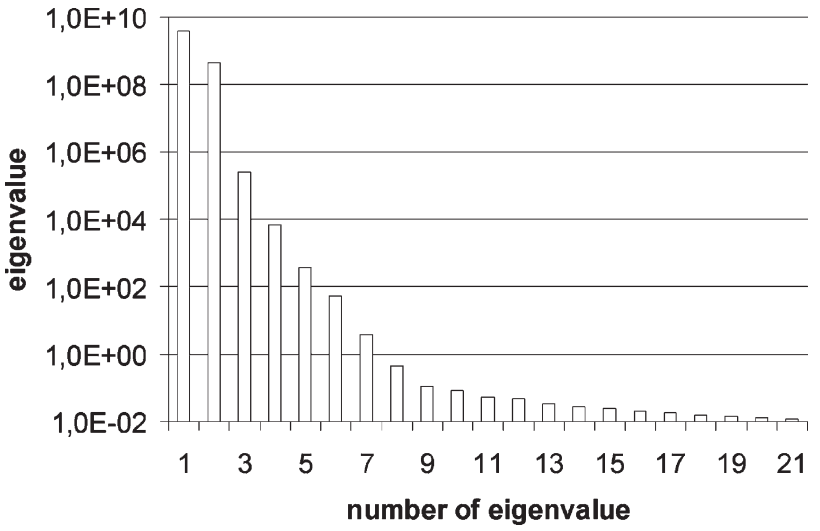

Figure 8. Distribution of eigenvalues of the covariance matrix for Example 3.

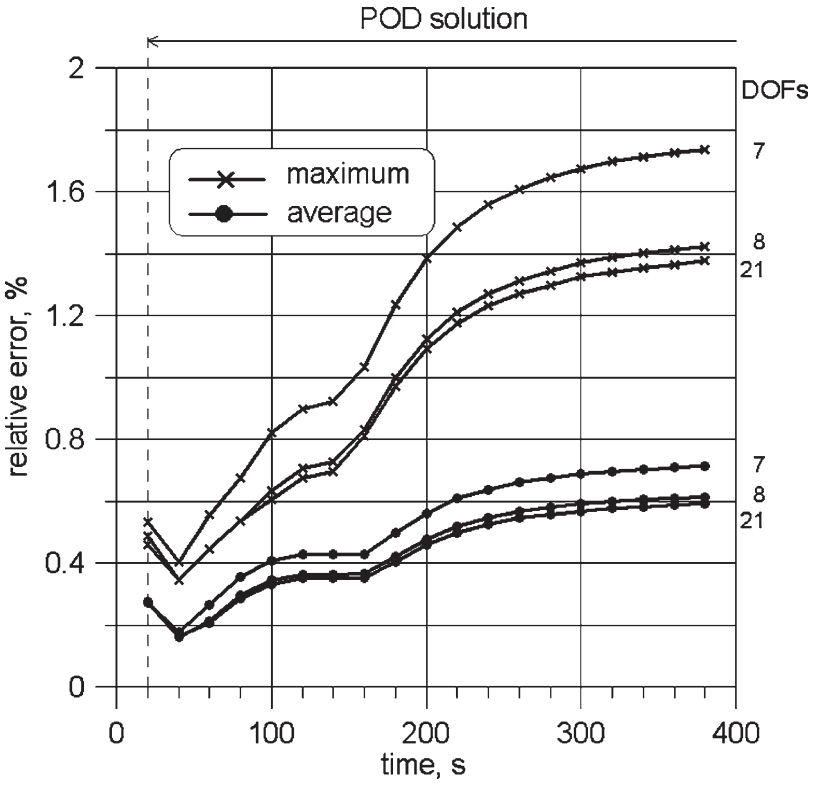

Figure 9. Errors of results obtained for Example 3 when POD basis with different values of DOFs was used. Numbers on the right margin indicate the numbers of DOFs.

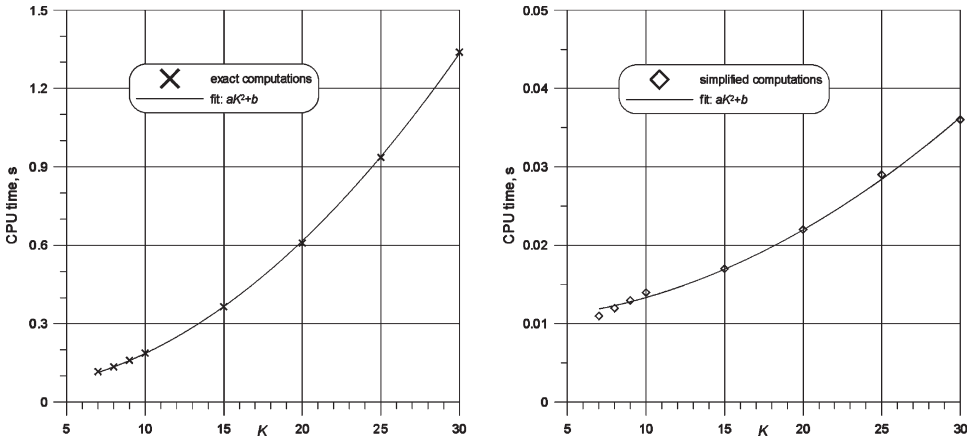

Figure 10. CPU time for assembly of volumetric components of matrix $\hat{\mathbf{K}}$ in a simplified and an exact way for Example 2.

with material properties evaluated at every Gaussian node, using the concept of average material properties decreases the assembly time of the $\hat{\mathbf{K}}$ matrix significantly. For the case of four Gaussian nodes/element used in the examples, the acceleration is between 4 and 10 times, depending on the number of POD modes. This can be clearly seen by comparing the execution times in Figure 10 and Table 1. It should be stressed that the simplification does not influence the accuracy of the final results. The differences between the temperature fields obtained using the simplified and rigorous matrix generation were in all cases considered below 0.2%.

The same averaging procedure applied to the standard FEM matrix does not lead to such a CPU time economy in the assembly process. Thus, the number of

Table 1 Processor times (s) for different operations within a single time step for Examples 2 and 3 with 8 DOFs using time-stepping POD-FEM

	Example 2		Example 3	
Operation	FEM	POD-FEM	FEM	POD-FEM
Assembling capacitance matrix $\mathbf{M}$ or $\hat{\mathbf{M}}$	0.03	0.04	0.44	0.79
Assembling volumetric component of conductance matrix $\mathbf{K}$ or $\hat{\mathbf{K}}$ exactly	0.08	0.14	0.98	1.80
Assembling volumetric component of matrix $\mathbf{K}$ or $\hat{\mathbf{K}}$ in a simplified way	0.02	0.01	0.21	0.18
Assembling boundary components of matrices $\mathbf{K}$ and $\mathbf{F}$ or $\hat{\mathbf{K}}$ and $\hat{\mathbf{F}}$	<0.005	0.01	0.01	0.05
Remaining operations while building final set of algebraic equations	0.03	<0.005	0.71	<0.005
Solving set of algebraic equations	0.03	<0.005	3.92	<0.005
Single time step				
$\mathbf{K}$ or $\hat{\mathbf{K}}$ calculated exactly	0.14[a]	0.16[a]	6.06	2.64
$\mathbf{K}$ or $\hat{\mathbf{K}}$ calculated approximately	0.08[a]	0.02[a]	5.29	1.02

[a]Capacitance matrix was calculated only once.

Table 2 Computing times for Examples 2 and 3

	Example 2		Example 3	
Kind of calculations	No. of DOFs	Time (s)	No. of DOFs	Time (min)
FEM	3,151	321.0	37,732	445.2
Snapshots generation		20.3		24.4
POD basis generation	31	8.5	21	3.1
Time-stepping POD-FEM	31	178.4	21	201.7
	11	92.4	10	72.5
	8	81.0	8	65.5
	7	77.0	7	62.2

nodes at which the POD-FEM brings execution time economy is lower if the simplified generation of matrices $\mathbf{K}$ and $\hat{\mathbf{K}}$ is used. For Example 2, with a small number of unknowns, the time-stepping POD-FEM technique with exact evaluation of matrix $\hat{\mathbf{K}}$ did not yield any gain in computing time. The savings in equation solving were compensated by the higher cost of the assembly. This is true even if a small but acceptable number of POD DOFs is applied (8 DOFs). The POD-FEM with simplified matrix generation leads to significant execution-time reduction.

The saving is more pronounced for larger problems (Example 3), as then the cost of equations solving becomes dominant. The computing time for solving sets of algebraic equations increases in the FEM with the growth of the number of nodes $[O(N^2)]$ much more quickly than the assembly process $[O(N)]$ [1]. Simultaneously, the cost of algebraic equations solving in the POD-FEM $[O(K^3)]$ does not depend practically on the number of nodes N, while the cost of assembly $[O(NK^2)]$ increases versus the growth of N comparatively as in the standard FEM.

Comparison of total computing times of Examples 2 and 3 is presented Table 2. The codes were run on a Pentium 4, 2.2 GHz, with 1 GB RAM. The simplified method of calculation of volumetric components of matrices for the POD-FEM (matrix $\hat{\mathbf{K}}$) based on Eq. (27) and the standard FEM (matrix $\mathbf{K}$) was applied in the time-stepping procedure. The mass matrix $\hat{\mathbf{M}}$ [Eq. (22)] was assembled in an exact way.

If the number of DOFs in the time-stepping POD-FEM technique is selected at a reasonable level (8–10 in Examples 2 and 3), the gain in the overall computational time (taking into account snapshots and basis generation) is of the order of 3–5 times. Further decrease of this time can be achieved using a simplified assembling procedure also for the mass matrix $\hat{\mathbf{M}}$.

The computational time in the time-stepping POD-FEM method depends strongly on the number of DOFs. Thus, this number should be selected carefully. If it is selected too high, the proposed technique cannot yield any execution time saving. On the other hand, too low a number of DOFs leads to unacceptable errors.

4.5. Error Estimation

Working with the truncated POD basis introduces some error. A simple means of assessing the error introduced by this approximation is an important question in practical applications. Recalling that access to the original stiffness and mass

matrices as well as the load vector is available, the POD solution obtained at a given time instant may be substituted into the original set of ODEs (17). The necessary temporal differentiation can be carried out numerically. The residuum of the original set of equations (17) can then be readily calculated at an arbitrary time instant. The norm of the residuum is frequently taken as a measure of the error in the case of iterative solvers, but the physical interpretation of such error is difficult.

The question that arises is how to relate two measures of the error: the residuum (which can be readily evaluated but does not have a direct physical meaning), and the error in nodal temperatures, which is the quantity of interest, but no plausible technique for its evaluation is available. Intuitively, these two measures should be closely related, hence the idea of assessing the error in temperatures by investigating the residuals arises in a natural way. Numerical tests indicate that

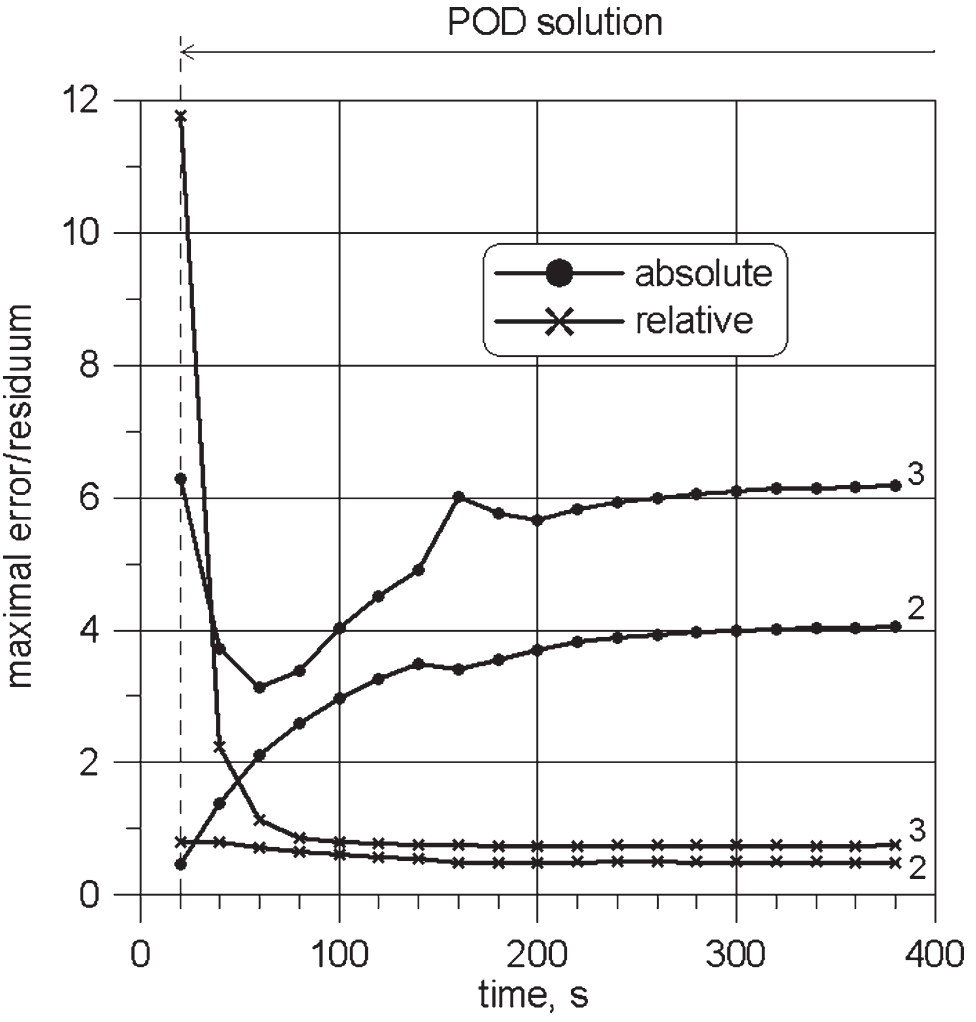

Figure 11. Ratio of maximum error and norm of residuals for Examples 2 and 3.

the ratio of these two error indicators remains practically at the same order of magnitude in time. Specifically, this is true in the case of the maximum absolute error $[\max_i(\delta T_i)]$. This is shown in Figure 11, which presents results for Examples 2 and 3 for 8 POD degrees of freedom.

5. CONCLUSIONS

The main reason for dealing with POD in the FEM context is the potential for reducing computing times. In the case of modal analysis and medium-size problems (60,000 DOFs), the technique leads to time economy of one order of magnitude [5]. In this case the stiffness and mass matrices are generated only once, and so are their POD-FEM counterparts. Moreover, the solution of the reduced ODEs is carried out analytically. In the case of nonlinear problems, the time saving is not that pronounced. The reason is that the POD-FEM matrices need to be recalculated at every time step. Thus, additional cost of multiplication of the FEM matrix by the POD basis is incurred at every time step. On the other hand, the system matrices to be factored are of significantly lower dimensionality. In the example under consideration, the time economy is of the order of 3–4. As the cost of solution increases faster than the cost of the matrix assembly, it can be predicted that the gain in using POD for larger problems will increase.

The main result of this study is the development for a technique for applying POD to nonlinear cases. Another important conclusion is that the error incurred by the truncated POD basis is (at least in the problem under consideration) at an acceptable level of 1%. It is worth noting that the POD basis need not be recalculated.

Additional gains in execution time can be expected. As shown in the case of hyperbolic equations [2], the POD-FEM equations can be solved using much larger time steps. This issue will be a topic of further research.

REFERENCES

1. P. Krysl, S. Lall, and J. E. Marsden, Dimensional Model Reduction in Non-linear Finite Element Dynamics of Solids and Structures, *Int. J. Numer. Meth. Eng.*, vol. 51, pp. 479–504, 2001.
2. P. A. LeGresley and J. J. Alonso, Investigation of Non-linear Projection for POD Based Reduced Order Models for Aerodynamics, AIAA Paper 2001-0926, presented at 39th AIAA Aerospace Science Meeting & Exhibit, Reno, NV, January 8–11, 2001.
3. D. Ahlman, F. Söderlund, J. Jackson, A. Kurdila, and W. Shyy, Proper Orthogonal Decomposition for Time-Dependent Lid-Driven Cavity Flows, *Numer. Heat Transfer B*, vol. 42, pp. 285–306, 2002.
4. R. A. Białecki, A. J. Kassab, and A. Fic, Reduction of the Dimensionality of Transient FEM Solutions Using Proper Orthogonal Decomposition, *Proc. 36th AIAA Thermophysics Conf.*, Orlando, FL, AIAA Paper, 2003–4207, 2003.
5. R. A. Białecki, A. J. Kassab, and A. Fic, Proper Orthogonal Decomposition and Modal Analysis for Acceleration of Transient FEM Thermal Analysis, *Int. J. Numer. Meth. Eng.*, vol. 62, pp. 774–797, 2005.
6. L. Sirovich, Turbulence and Dynamics of Coherent Structures, Part I: Coherent Structures, *Q. Appl. Math.*, vol. XLV, pp. 561–571, 1987.

7. Y. C. Liang, H. P. Lee, S. P. Lim, W. Z. Lin, K. H. Lee, and C. G. WU, Proper Orthogonal Decomposition and Its Applications—Part I: Theory, *J. Sound Vibration*, vol. 252, no. 3, pp. 527–544, 2002.
8. K. Pearson, On Lines Planes of Closes Fit to System of Points in Space, *London Edinburgh Dublin Phil. Mag. J. Science*, vol. 2, pp. 559–572, 1901.
9. H. Hotelling, Analysis of Complex of Statistical Variables into Principal Components, *J. Educ. Psych.*, vol. 24, pp. 417–441, 1933.
10. K. Karhunen, Ueber lineare Methoden füer Wahrscheinigkeitsrechnung, *Ann. Acad. Sci. Fennicae Ser. A1 Math. Phys.*, vol. 37, pp. 3–79, 1946.
11. M. M. Loeve, *Probability Theory*, Van Nostrand, Princeton, NJ, 1955.
12. M. Kirby and L. Sirovich, Application of Karhunen-Loeve Procedure for Characterization of Human Faces, *IEEE Trans. Pattern Anal. Machine Intell.*, vol. 12, no. 1, pp. 103–108, 1990.
13. J. A. Atwell and B. B. King, Proper Orthogonal Decomposition for Reduced Basis Feedback Controllers for Parabolic Equations, *Math. Comput. Modell.*, vol. 33, pp. 1–19, 2001.
14. K. S. Ball, L. Sirovich, and L. R. Keefe, Dynamical Eigenfunction Decomposition of Turbulent Channel Flow, *Int. J. Numer. Meth. Fluids*, vol. 12, pp. 585–604, 1991.
15. V. R. Algazi, K. L. Brown, and M. J. Reddy, Transform Representation of the Spectra of Acoustic Speech Segments with Applications, Part I: General Approach and Application to Speech Recognition, *IEEE Trans. Speech Audio Process.*, vol. 1, pp. 180–195, 1993.
16. S. A. Zahorian and M. Rothenberg, Principal Component Analysis for Low-Redundancy Encoding of Speech Spectra, *J. Acoust. Soc. Am.*, vol. 69, pp. 519–524, 1981.
17. Z. Nenadic, B. K. Gosh, and P. S. Ulinski, Modelling and Estimation Problems in the Turtle Visual Cortex, *IEEE Trans. Biomed. Eng.*, vol. 49, no. 8, pp. 753–762, 2002.
18. R. B. Białecki, A. J. Kassab, and Z. Ostrowski, Application of the Proper Orthogonal Decomposition in Steady State Inverse Problems, in M. Tanaka and G. S. Dulikravich (eds.), *Proc. Int. Symp. on Inverse Problems in Engineering Mechanics*, Nagano City, Japan, 3–12, Elsevier, Amsterdam, Boston, 2003.
19. *Fortran Subroutines for Mathematical Applications Math/Library Volumes 1 and 2*, Visual Numerics, 1997. Electronic documentation: www.vni.com/books/docs.
20. H. V. Ly and H. T. Tran, Modeling and Control of Physical Processes Using Proper Orthogonal Decomposition, *Math. Comput. Modell.*, vol. 33, pp. 223–236, 2001.
21. O. C. Zienkiewicz and R. L. Taylor, *The Finite Element Method*, vol. 1, McGraw-Hill, London and New York, 1989.